Generating Optical Schrödinger Kittens for Quantum Information Processing

Alexei Ourjoumtsev, Rosa Tualle-Brouri, Julien Laurat, Philippe Grangier

Generating Optical Schrödinger Kittens
for Quantum Information Processing

A. Ourjoumtsev, R. Tualle-Brouri, J. Laurat and P. Grangier

We present a detailed experimental analysis of a free-propagating light pulse prepared in a "Schrödinger kitten" state, defined as a quantum superposition of "classical" coherent states with small amplitudes. This state is generated by subtracting one photon from a squeezed vacuum beam, and it clearly presents a negative Wigner function. The predicted influence of the experimental parameters is in excellent agreement with the experimental results. The amplitude of the coherent states can be amplified to transform our "Schrödinger kittens" into bigger Schrödinger cats, providing an essential tool for quantum information processing.

A key requirement for many quantum computation and communication protocols (*1, 2*) is to dispose of specific quantum states of light as a resource for information processing. In the following, we will be interested in quantum states of propagating light beams, which can be analyzed either by photon counting, or by homodyne detection, which measures the interference between the signal state and an intense reference beam with a relative phase θ. This measures a physical quantity called a "quadrature component" of the electric field, associated with the operator $\hat{x}_\theta = \hat{x}cos\theta + \hat{p}sin\theta$, where $\hat{x}$ and $\hat{p}$ are canonically conjugate field observables. The operators $\hat{x}$ and $\hat{p}$ are analog to the position and the momentum of a particle, and they are often called "quantum continuous variables" (QCV). From Heisenberg's inequalities they cannot be determined simultaneously with an infinite precision, so one cannot generally define a proper phase-space density $\Pi(x, p)$ for the electric field. However, one can define a quasi-distribution $W(x, p)$ called the Wigner function, the marginals of which yield the probability distributions $P(x_\theta)$. By measuring the distributions $P(x_\theta)$ for several values of θ one can reconstruct the Wigner function; this inverse process is known as quantum tomography (*3*).

For specific quantum states, the Wigner function can take negative values, thereby excluding any description by a classical phase-space density. Generating such states for propagating light beams is of special interest for QCV information processing, because it provides the basis for entanglement distillation (*4–6*), universal quantum computing (*7–9*), and proposed loophole-free tests

of Bell's inequalities (*10,11*). Such states have been realized recently by combining homodyne detection with photon counting, so that the quadrature components are measured only when a photon is detected in another (triggering) channel (*12–16*). We have shown recently that one can "degaussify" a squeezed state of the light, and turn it into a state with a Wigner function which was observed to be strongly non-gaussian, though still positive (*14, 17, 18*). Here we experimentally observe a propagating light field which exhibits a negative valued Wigner function and is very close to a "small" Schrödinger cat state.

Among non-classical states, Schrödinger cat states play an especially interesting role. Defined as quantum superpositions of classical distinguishable states, they are very useful to study the process of decoherence involved in the transition from quantum to classical physics (*19*), which strongly limits the development of quantum computing and communications. Coherent states are the most "classical" available in quantum physics, and we will call a Schrödinger cat state a quantum superposition of coherent states, well separated in phase space, for example $|\psi\rangle = c(|\alpha\rangle - |-\alpha\rangle)$, where $|\alpha|$ is the amplitude of the coherent states and c is a normalization factor. In this case, $|\alpha|^2$ defines the "size" of the cat, which becomes a "Schrödinger kitten" when $|\alpha|^2$ is small. The Wigner function of such a state presents a negative value at the origin. Here we wish to generate free-propagating optical Schrödinger kittens which, unlike Schrödinger cats generated in cavities or bound systems (*19–21*), can be used for quantum communica-

tions. Such kittens can be produced with a very high fidelity either by subtracting one photon from a squeezed vacuum state (*22*) (see Fig. 1), or by squeezing one photon (*8, 23*). The subtraction procedure, simpler to implement, can be realized by reflecting towards an avalanche photodiode (APD) a small fraction of a squeezed vacuum beam produced by a degenerate optical parametric amplifier. The APD will herald the subtraction of at least one photon, and the probability to subtract more than one photon will become negligible for a low reflectivity. Thus, an APD detection will project the transmitted beam into the desired state.

Fig. 1. Wigner function of an ideal photon-subtracted squeezed state ($s = 0.6$) (left), compared to the one of the closest Schrödinger kitten ($|\alpha_{opt}|^2 = 0.8$) (right). For any value of $|\alpha|^2 < 1$, the theoretical fidelity between the two matched states is larger than 0.997)
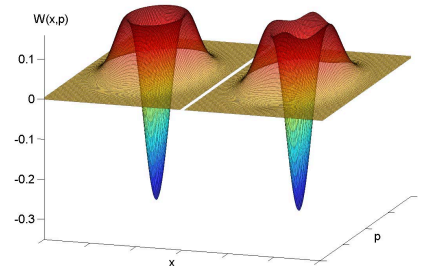
In our experiment (Fig. 2), a squeezed vacuum beam is produced in a frequency-degenerate optical parametric amplifier (DOPA) by down-conversion of frequency-doubled femtosecond laser pulses (see supporting online text). A beamsplitter reflects 9.5% of the squeezed beam towards an APD through a filtering system, whereas the

transmitted beam is analyzed by a homodyne detection. This detection works in a time-resolved regime, and measures one quadrature $\hat{x}_\theta$ for each incoming pulse.

Quantum superpositions are very fragile, and four main sources of decoherence appear in our case. First, the state conditioned by the APD must belong to the spatio-temporal mode analyzed by the homodyne detection. We will consider that it actually belongs to this mode with a probability ξ, and to an orthogonal mode with a probability $1 - \xi$. This modal purity parameter ξ is decreased by the limited spatial and spectral quality of the optical beams, by the imperfections of the filtering system, and by the APD dark counts. These effects mix the ideal photon-subtracted state with a non-conditioned squeezed state. The experiment is also extremely sensitive to excess noise from the DOPA, which can be modelled by introducing a second, phase-independent optical amplifier with a gain $h = cosh^2(\gamma r_s)$ after an ideal degenerate amplifier squeezing the quantum noise variance by a factor $s = exp(-2r_s)$. A non-zero γ, which defines the ratio between the efficiencies of the two amplification processes, adds uncorrelated APD counts and homodyne noise. Furthermore, the reflectivity R of the pickup beamsplitter has to be large enough to ensure a count rate much above the dark counts of the APD. Therefore it introduces finite losses on the transmitted beam, mixing it with vacuum. Finally, two defects appear on the homodyne detection side : the limited homodyne detection efficiency η, and the electronic noise e (normalized to the shot-noise value). However, these defects are not involved in the generation but only in the characterization of the state. They can be estimated independently, and corrected for in order to determine the Wigner function of the prepared state. All of these parameters are extremely critical, and every percent of losses strongly deteriorates the state. Generating states with negative Wigner functions required to adjust very carefully the filtering system and to pay a special attention to the wavefront quality of the beams, in particular during the extraction of the pulses from the laser cavity and during the frequency-doubling process. An optimized homodyne detection design allowed to observe negative values without correcting for detection losses (24).

Fig. 2 Experimental setup, and reconstructed Wigner function of the photon-subtracted squeezed vacuum ("Schrödinger's kitten") propagating in the experiment ($s = 0.56$, corrected for homodyne losses).
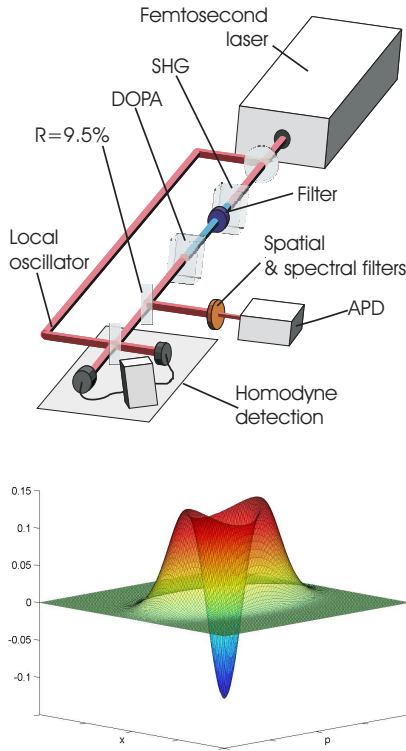
We show in the supporting online text that in realistic and quite general experimental conditions the Wigner function and the marginal distributions of the detected state have very simple analytic expressions parameterized by four quantities $\sigma_1(s)$, $\sigma_1(1/s)$, $\sigma_2(s)$, $\sigma_2(1/s)$, functions of the experimental parameters introduced above. This model allows not only for theoretical predictions, but also for a very efficient data analysis, since these quantities can be extracted from the second and fourth moments of the measured distributions $P_{exp}(x_\theta)$ with a simple algebraic procedure.

We generated and characterized three "kittens" of different sizes defined by squeezing factors $s_1 = 0.56$, $s_2 = 0.60$ and $s_3 = 0.63$. For each of them, a quantum tomography was performed by measuring six quadrature distributions $P_{exp}(x_\theta)$ for $0 \le \theta \le 5\pi/6$. For each value of θ, approximately 20000 experimental points were acquired and divided into 64-bin histograms. The analysis procedure described above provides, without any free parameter, an excellent fit to the data (Fig. 3), as well as a simple analytical expression for the (raw data) Wigner function. The Wigner function reconstructed using this method is in very good agreement with the one obtained from the model-independent Radon transform (Fig. 3), applied to the uncorrected experimental data. In addition, our procedure provides values for all experimental parameters, which are found to be fully consistent with the values directly measured on the experiment (see Table 1).

Fig. 3. (A) Experimentally measured quadratures and theoretical fits, corresponding to a squeezing factor $s = 0.56$. (B) Wigner function obtained by the generic model described online. (C) Wigner function obtained by Radon transform of the raw experimental data. In all these curves no correction is made for detection efficiencies, which are included in the generic model together with other imperfections (see text for details).
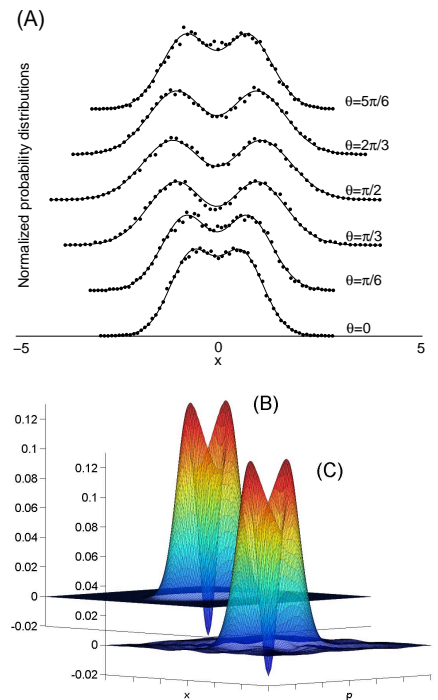
It is clear from Fig. 3 that these measurements provide a negative value

for the uncorrected Wigner function, $W_{raw}(0) = -0.026 \pm 0.012$, while this was not the case in ref. 14. The quality of the above fits gives confidence that the experimental parameters provided by our analysis procedure are correct. In order to determine the Wigner function of the generated state, we have to correct for the effect of a limited homodyne detection efficiency η and an excess noise e. This can be done by the standard maximal-likelihood method (*25, 26*), but we checked that the very same results are obtained immediately from our model : we simply replace the values of η and e determined from our data by $\eta = 1$ and $e = 0$ in the expression of the Wigner function. All the other parameters, involved in the generation process, are kept unchanged. The resulting Wigner function for $s = 0.56$ is displayed on Fig. 2, showing a very strong negativity $W_{cor}(0) = -0.13 \pm 0.01$. This is to be compared with -0.32 for a perfect setup with an infinitely low BS reflectivity, and -0.25 for a reflectivity of 9.5% and $s = 0.56$.

The reconstructed state is similar to a Schrödinger kitten of size $|\alpha|^2 = 0.79$, with a fidelity $F_{cat} = 70\%$. Clearly it is still a statistical mixture, mostly due to the conditioning process, which is not corrected here since it is involved in the generation of the state. It can thus be decomposed further in pure states, and simple calculations show that it can be written as 70% of the ideal photon-subtracted state, 29% of the initial squeezed state, and 1% of residuals. If our state was a purely statistical mixture of coherent states, this fidelity would be 0.40, and would remain below 0.50 for any $|\alpha|^2$. The results for the various experimental values of s are presented in Table 1.

The present procedure allows to reproduce small Schrödinger kittens, but the structure of a larger cat becomes more complicated (*24*). For "growing the cat", the generated kitten's state should be taken as a starting point to initiate a "breeding" process as described by Lund et al. (*23*). This can be done by combining two kitten states of a beamsplitter, and using one output channel for another photon-counting "purifying" measurement, while the other channel provides the cat state with a larger amplitude. As the quality of our state is actually higher than it was assumed in ref. 23, such an experiment can be realistically envisioned. Our setup also allows, with minor modifications, to generate quadrature-entangled pulses (*27*). Subtracting one photon from each mode provides entangled beams with negative Wigner functions, which have been proposed to improve the fidelity of continuous-variable teleportation (*28–30*), and to implement a loophole-free Bell test (*10, 11*). These examples clearly show that the availability of the states demonstrated here opens the way to many new quantum information and communication protocols.

Table 1. Analysis of the generated states, after correction for the homodyne efficiency $\eta = 80\%$ and electronic noise $e < 0.04$ shot noise units. There is no correction for the excess noise factor γ and the modal purity ξ (the values presented above are directly obtained from the fitting procedure). Here s is the squeezing factor, $W(0)$ is the Wigner function negativity, F_{vac} is the fraction of initial squeezed state, F_{cat} is the fidelity with the most similar Schrödinger kitten of size $|\alpha_{opt}|^2$. As expected, in this range of parameters the size of the kitten increases when the initial state is more and more squeezed (smaller s).

s	$W(0)$	F_{vac}	F_{cat}	$|\alpha_{opt}|^2$	γ	ξ
0.56	-0.13 ± 0.01	29%	70%	0.79	0.17	0.82
0.60	-0.09 ± 0.01	35%	64%	0.71	0.47	0.89
0.63	-0.08 ± 0.01	36%	63%	0.62	0.45	0.86

References and Notes

1. M. A. Nielsen, I. Chuang, *Quantum computation and quantum information* (Cambridge University Press, Cambridge, 2000).

2. C. H. Bennett, D. P. Di Vincenzo, *Nature* **404**, 247 (2000).

3. K. Vogel, H. Risken, *Phys. Rev. A* **40**, 2847 (1989).

4. J. Eisert, S. Scheel, M. B. Plenio, *Phys. Rev. Lett.* **89**, 137903 (2002).

5. G. Giedke, J. I. Cirac, *Phys. Rev. A* **66**, 032316 (2002).

6. D. E. Browne, J. Eisert, S. Scheel, M. B. Plenio, *Phys. Rev. A* **67**, 062320 (2003).

7. A. Gilchrist *et al.*, *J. Opt. B: Quantum Semiclass. Opt.* **6**, S828 (2004).

8. H. Jeong, T. C. Ralph, *Arxiv:quant-ph/0509137, to be published in "Quantum Information with Continuous Variables of Atoms and Light" (Imperial College Press)* (2005).

9. S. D. Bartlett, B. C. Sanders, *Phys. Rev. A* **65**, 042304 (2002).

10. R. García-Patrón *et al.*, *Phys. Rev. Lett.* **93**, 130409 (2004).

11. H. Nha, H. J. Carmichael, *Phys. Rev. Lett.* **93**, 020401 (2004).

12. S. Song, C. Caves, B. Yurke, *Phys. Rev. A* **41**, 5261 (1990).

13. A. I. Lvovsky *et al.*, *Phys. Rev. Lett.* **87**, 050402 (2001).

14. J. Wenger, R. Tualle-Brouri, P. Grangier, *Phys. Rev. Lett.* **92**, 153601 (2004).

15. A. Zavatta, S. Viciani, M. Bellini, *Phys. Rev. A* **70**, 053821 (2004).

16. J. Fiurášek, R. García-Patrón, N. J. Cerf, *Phys. Rev. A* **72**, 033822 (2005).

17. M. S. Kim, E. Park, P. L. Knight, H. Jeong, *Phys. Rev. A* **71**, 043805 (2005).

18. S. Olivares, M. G. A. Paris, *arXiv:quant-ph* p. 0506108 (2005).

19. M. Brune *et al.*, *Phys. Rev. Lett.* **77**, 4887 (1996).

20. B. Yurke, D. Stoler, *Phys. Rev. Lett.* **57**, 13 (1986).

21. C. Monroe, D. M. Meekhof, B. E. King, D. J. Wineland, *Science* **272**, 1131 (1996).

22. M. Dakna, T. Anhut, T. Opatrný, L. Knöll, D.-G. Welsch, *Phys. Rev. A* **55**, 3184 (1997).

23. A. P. Lund, H. Jeong, T. C. Ralph, M. S. Kim, *Phys. Rev. A* **70**, 020101(R) (2004).

24. Materials and methods are available as supporting material on Science Online.

25. J. Řeháček, Z. Hradil, M. Ježek, *Phys. Rev. A* **63**, 040303(R) (2002).

26. A. I. Lvovsky, *J. Opt. B: Quantum Semiclass. Opt* **6**, S556 (2004).

27. J. Wenger, A. Ourjoumtsev, R. Tualle-Brouri, P. Grangier, *Eur. Phys. J. D* pp. 391–396 (2005).

28. T. Opatrný, G. Kurizki, D.-G. Welsh, *Phys. Rev. A* **61**, 032302 (2000).

29. P. T. Cochrane, T. C. Ralph, G. J. Milburn, *Phys. Rev. A* **65**, 062306 (2002).

30. S. Olivares, M. G. A. Paris, R. Bonifacio, *Phys. Rev. A* **67**, 032314 (2003).

31. This work was supported by the EU project COVAQIAL.